

Supplementary Information

Topological surface states induced by the magnetic proximity effect

Soichiro Fukuoka, Le Duc Anh, Masayuki Ishida, Tomoki Hotta, Takahiro Chiba, Yohei*

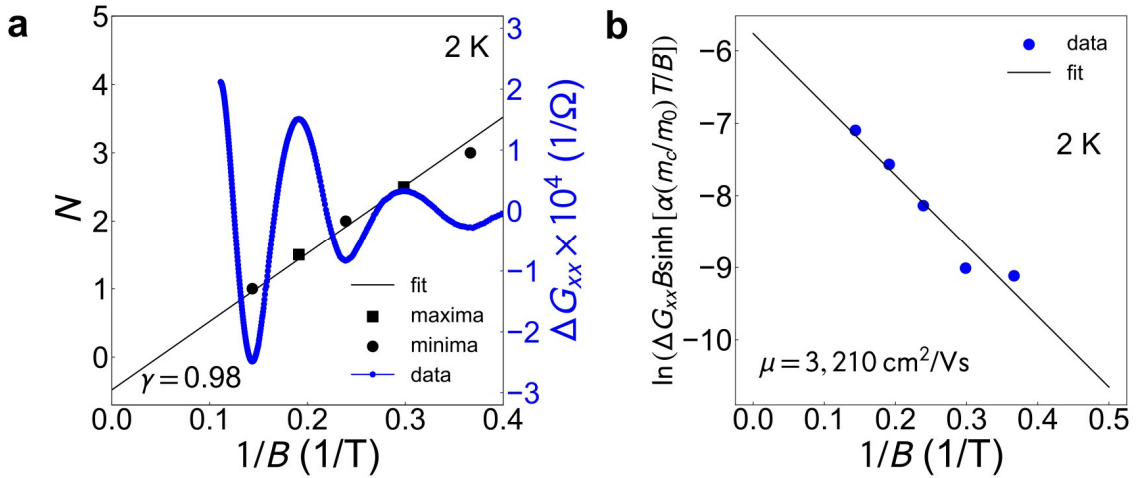
*Kota, and Masaaki Tanaka**

Supplementary Note 1. The Dingle and fan diagram plots of the reference sample

We independently determined μ and γ in the reference sample using a standard Dingle plot with Equation (S1) and a fan plot with Equation (S2), respectively, as shown in Figure S1. The fan plot shows a phase shift of 0.98, which is consistent with the result of 0.97 in Figure. 3d. Additionally, the mobility was estimated to be 3,210 cm²V⁻¹s⁻¹ from the Dingle plot, which also agrees with the result of 2,820 cm²V⁻¹s⁻¹ in Figure. 3d.

$$\ln \left(\frac{\Delta G}{\left(\frac{2\pi^2 k_B T}{\hbar \omega} \right) \sinh \left(\frac{2\pi^2 k_B T}{\hbar \omega} \right)} \right) = -\frac{\pi}{q\mu} \frac{1}{B} + C \quad (\text{S1})$$

$$2\pi \left(\frac{F}{B} - \gamma \right) = (2N - 1)\pi \quad (\text{S2})$$



Supplementary Figure S1. (a) Fan plot of the component F . The blue line represents the oscillatory part. The minima (black circles) and maxima (black squares) are estimated from the fitting curve. By this fitting the phase γ is estimated as 0.98. (b) Dingle plot of the component F , where α is $2\pi^2 k_B m_0 / \hbar q \sim 14.7$. By fitting the Equation (3) (black line) to the experimental data (blue circles), the quantum mobility μ is estimated to be 3,210 cm²V⁻¹s⁻¹.

Supplementary Note 2: Estimation of the Fermi level E_F in the reference sample

Since the band corresponding to the comment F exhibits linear dispersion, the distance from the Dirac point to the Fermi level E_F takes the following value.

$$|E_F - E_{DP}| = \frac{2\hbar q}{m} F = 21.1 \text{ meV} \quad (\text{S3})$$

Additionally, as the carrier type of α -Sn thin film tends to be p-type, we consider that the Fermi level is located at the position shown in Figure. 3e.

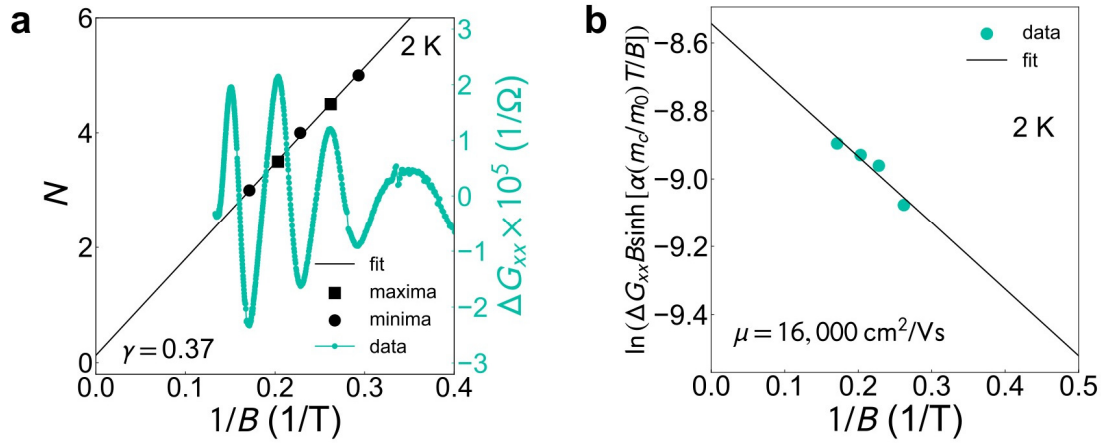
Supplementary Note 3: Dingle and fan diagram plots of the $\text{FeO}_x/\text{FeAs}/\alpha\text{-Sn}$ heterostructure

We independently determined μ and γ of the component F_{Low} in the $\text{FeO}_x/\text{FeAs}/\alpha\text{-Sn}$ heterostructure using a standard Dingle plot with Equation (S1) and a fan plot with Equation (S2), respectively. To extract only the low-frequency band F_{Low} , measurements up to 9 T were performed. Based on the analysis shown in Figure. 4, where $\mu_{\text{High}} = 1,040 \text{ cm}^2\text{V}^{-1}\text{s}^{-1}$, the condition for observing quantum oscillations

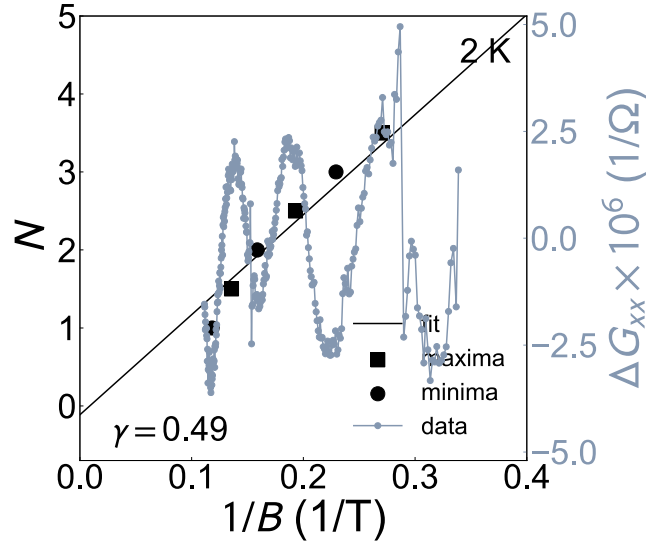
$$\mu B_c \sim 1 \quad (\text{S4})$$

allows us to determine that the magnetic field B_c at which quantum oscillations of the band begin to appear is about 10 T. In other words, it is expected that quantum oscillations of the F_{High} band would not be observed in measurements up to 9 T.

As shown in Figure. S2, the fan plot shows a phase shift of $\gamma = 0.37$, which is consistent with the result of $\gamma = 0.28$ in Figure. 4c. Additionally, the mobility μ was estimated to be $16,000 \text{ cm}^2\text{V}^{-1}\text{s}^{-1}$ from the Dingle plot. This is also consistent with the fitting results using a summation of multiple components explained in the main manuscript (Figure. 4), demonstrating the reliability of the fitting approach. Note that due to the time gap between measurements in Figure. 4c and Figure. S2, there may be variations in sample quality, resulting in slightly different values from the fitting.



Supplementary Figure S2. (a) Fan plot of the component F_{Low} . The green curve represents the oscillatory part. The minima (black circles) and maxima (black squares) are estimated from the fitting curve. By this fitting, the phase γ is estimated to be 0.37. (b) Dingle plot of the component F , where α is $2\pi^2 k_B m_0 / \hbar q \sim 14.7$. By fitting the Equation (S1) (black line) to the experimental data (green circles), the quantum mobility μ is estimated to be $16,000 \text{ cm}^2 \text{V}^{-1} \text{s}^{-1}$.



Supplementary Figure S3. Fan plot of the component $F_{\text{in-plane}}$. The grey line represents the oscillatory part. The minima (black circles) and maxima (black squares) are estimated from the fitting curve. By fitting Eq (S1) to the experimental data, the phase γ is estimated to be 0.49.

Supplementary Note 4: Fan diagram plot of the $F_{\text{In-plane}}$ peak in the FeO_x/FeAs/ α -Sn heterostructure with a magnetic field angle $\theta = 90$ degree

As shown in Figure. S3, the phase shift γ of the $F_{\text{In-plane}}$ component was found to be 0.49, indicating parabolic dispersion. This suggests that it originates from a trivial band typical of conventional electronic systems. Since it exhibits 3D conduction, the band component likely belongs to InSb. Because the extremal orbit was assumed to be a maximum, we used $+1/8$ as δ in Equation (1) of the main manuscript when estimating γ .

Supplementary Note 5: Assignment of the bands in the FeO_x/FeAs/ α -Sn heterostructure for the components F_{High} and F_{Low}

From the results of band structure calculations, it is likely that the Fermi level crosses two bands, the top of HH band and the TSS, of the α -Sn layer. Based on this consideration, the wave number k of F_{Low} is $1.94 \times 10^6 \text{ cm}^{-1}$ and F_{High} is $3.19 \times 10^6 \text{ cm}^{-1}$, thereby the area of the Fermi surface of F_{High} is larger than that of F_{Low} . This leads to the assignments shown in Figure. 4 of the main text; F_{High} and F_{Low} correspond to HH and TSS, respectively. Furthermore, the high quantum mobility of F_{Low} and the parabolic dispersion of F_{High} also support the assignment.

Since F_{Low} exhibits linear dispersion, we can estimate the distance from the Dirac point to the Fermi level to be 17.2 meV, by using equation (S3). The Fermi level E_F was set from this value in Figures. 4f and g.

Supplementary Note 6: Characterization of the DFT results by 2D massless Dirac Hamiltonian interacting to magnetic moments

Here we characterize the TSS band structure obtained by the DFT calculations based on 2D massless Dirac Hamiltonian which gives a simple model for the electronic structure of a TSS. As shown in Figure. 4f, we model the TSS on the bottom surface of Sn as 2D massless Dirac electrons that are exchange-coupled to a homogeneous magnetization \mathbf{M} of FeAs via the magnetic proximity effect (MPE). Because of a very thin film of the Sn layer, we assume that MPE overcomes the slab system. Then, a low-energy effective Hamiltonian is given by ^[S1,S2]

$$\hat{H}_{2D} = -i\hbar v_F \hat{\sigma} \cdot (\nabla \times \hat{z}) + \Delta \hat{\sigma} \cdot \mathbf{M} \quad (\text{S5})$$

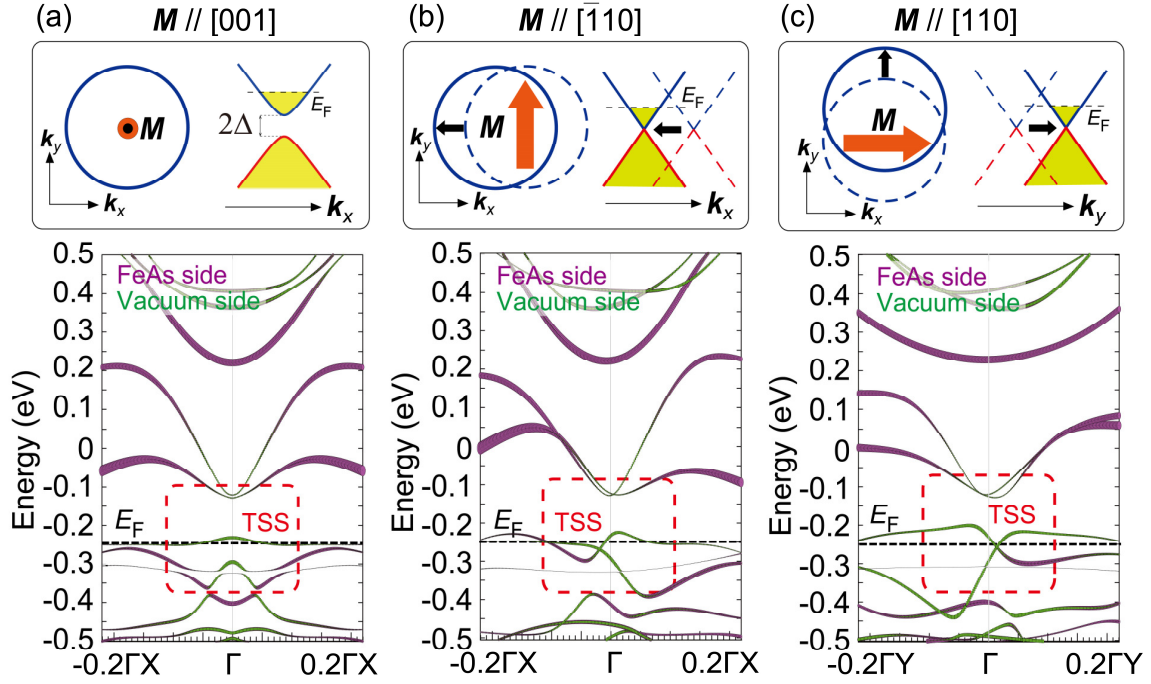
where \hbar is the reduced Planck constant, v_F is the Fermi velocity of the Dirac electrons, $\hat{\sigma}$ is the Pauli matrix operator, and Δ is the MPE-induced exchange energy that is responsible for the hybridization between s,p and d orbitals. The Hamiltonian (S5) leads to the energy-momentum dispersion

$$E_{\mathbf{k}s} = s \sqrt{\left(\hbar v_F k_x + \Delta M_y\right)^2 + \left(\hbar v_F k_y - \Delta M_x\right)^2 + \left(\Delta M_z\right)^2} \quad (\text{S6})$$

where $\hbar \mathbf{k}$ is the momentum measured relative to the Γ point of the 2D Brillouin zone and $s = \pm$ denotes the index of the upper (electron) and lower (hole) bands. The energy-momentum dispersion (S6) for fixed magnetization directions is schematically shown in Figure. S4 (top illustrations). As seen in Figure. S4 (bottom panels), the TSS band structure for the cases of $\mathbf{M} // [001]$, $\mathbf{M} // [\bar{1}10]$, $\mathbf{M} // [110]$ obtained by the DFT calculations are in excellent agreement with predictions by the Dirac electron model. Note that $\mathbf{M} // [\bar{1}10]$ and $\mathbf{M} // [110]$ directions correspond to M_y and M_x components in Eq. (S6), respectively.

Supplementary References

- [S1] K. Nomura and N. Nagaosa, "Electric charging of magnetic textures on the surface of a topological insulator," Phys. Rev. B **82**, 161401(R) (2010).
- [S2] T. Chiba, S. Takahashi, and G. E. W. Bauer, "Magnetic-proximity-induced magnetoresistance on topological insulators," Phys. Rev. B **95**, 094428 (2017).



Supplementary Figure S4. Illustrations of the topological surface state (TSS) (top panels) and calculated band structures along the $\Gamma - X$ (k_x) or $\Gamma - Y$ (k_y) axis (bottom panels) are shown for the cases of (a) $\mathbf{M} \parallel [001]$, (b) $\mathbf{M} \parallel [\bar{1}10]$, (c) $\mathbf{M} \parallel [110]$. The bottom panels show the projection of the calculated band components of the FeAs/ α -Sn heterostructure contributed from the Sn atoms at the interfaces with the top FeAs layer (purple) and the bottom vacuum surface (green) corresponding to the interface with InSb in our experiment. The vacuum surface states are concentrated in the topological gap (surrounded by the red dashed curve). The interface band structure of Sn changes drastically with the magnetisation direction (\mathbf{M}) of FeAs due to spin-momentum locking. When $\mathbf{M} \parallel [001]$, the TSS opens a small exchange gap of 2Δ at $(-0.15 \sim -0.3 \text{ eV})$ due to time reversal symmetry breaking. A linear TSS is observable when $\mathbf{M} \parallel [\bar{1}10]$ and $\mathbf{M} \parallel [110]$ as shown in b) and c), respectively, which is shifted away from the Γ point due to the spin-momentum locking and MPE.